Isokane et al., http://www.jcb.org/cgi/content/full/jcb.201408089/DC1

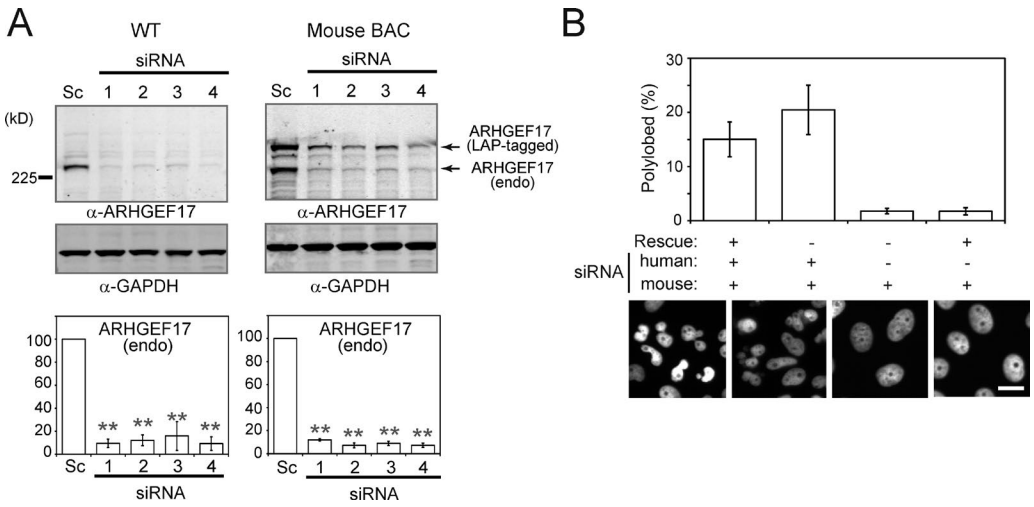

Figure S1. **Knockdown efficiency and rescue validation for ARHGEF17.** (A, top) Immunoblot analysis of endogenous hARHGEF17 in wild-type (WT; left) or LAP-mARHGEF17-BAC-expressing (right) HeLa Kyoto cells under si(Scrambled) (Sc) and si(hARHGEF17) knockdown detected by anti-ARHGEF17 antibodies. Numbers refer to oligonucleotide number (see Materials and methods). GAPDH was used as a loading control. (bottom) Quantification of protein knockdown of endogenous (endo) hARHGEF17. Bar graphs show mean ± SD of three independent experiments. **, $P < 0.01$ by two-tailed unpaired Student's *t* test compared with si(Scrambled).(B) Validation of siRNA knockdown and targeting of ARHGEF17 by phenotypic rescue experiment. (top) Bar plot comparing percentage of polylobed nuclei (normalized to Scrambled in each condition) in HeLa Kyoto cells stably expressing H2B-mCherry with or without LAP-mARHGEF17-BAC and treated with si(mARHGEF17) together with or without si(hARHGEF17) from >1,000 cells/three independent experiments. Bar graphs show mean ± SD.Cells were automatically segmented and analyzed by CellCognition software. (bottom) Images showing H2B-mCherry 48 h after siRNA transfection. Bars, 10 µm.

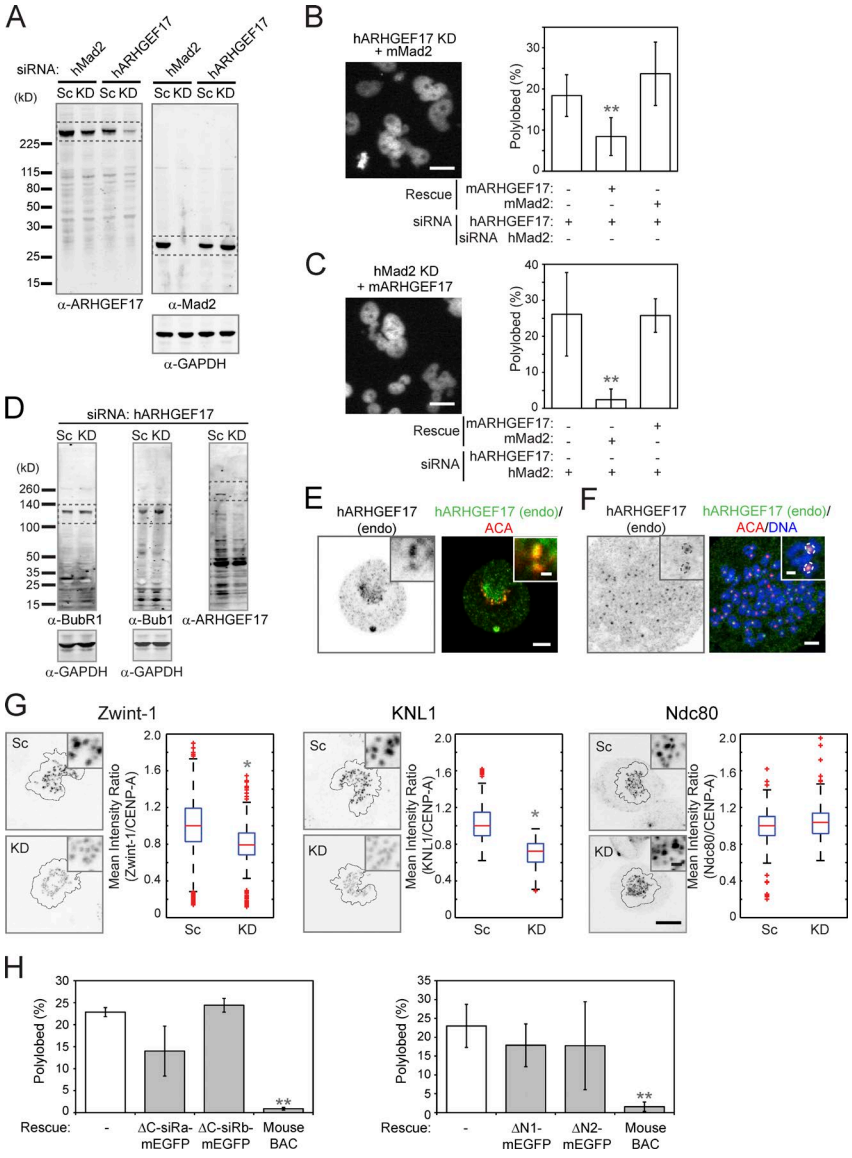

Figure S2. **Specificity of ARHGEF17 knockdown, effect on additional kinetochore protein targeting, ARHGEF17 kinetochore localization, and ARHGEF17 fragment rescue controls.** (A) Immunoblot analysis of endogenous hMad2 and endogenous hARHGEF17 48 h after siRNA transfection in si(Scrambled) (Sc), si(hARHGEF17), or si(hMad2) knockdown (KD) conditions detected by ARHGEF17 (left) and Mad2 (right) antibodies. GAPDH was used as a loading control. (B and C) (left) Images showing H2B-mCherry 48 h after siRNA transfection in si(hARHGEF17) (B) or si(hMad2) (C) knockdown in HeLa Kyoto cells stably expressing H2B-mCherry with or without LAP-mMad2-BAC (B) or LAP-mARHGEF17-BAC (C). Bars, 10 µm. (right) Bar plot comparing polylobed percentage from 5,600 cells/three independent experiments. Bar graphs show mean ± SD. Cells were automatically segmented and analyzed with CellCognition software. (D) Immunoblot analysis of the endogenous hBubR1 and hBub1 48 h after siRNA transfection in si(Scrambled) or si(hARHGEF17) knockdown conditions detected by BubR1 (left), Bub1 (middle), and ARHGEF17 (right) antibodies. GAPDH was used as a loading control. (E) Localization of endogenous hARHGEF17 in early mitotic HeLa Kyoto cell. Overlay shows hARHGEF17 (green) and ACA (red). Bars: (main) 5 µm; (inset) 0.5 µm. (F) Immunofluorescence images of endogenous hARHGEF17 on mitotic chromosomes. Prometaphase chromosome spreads of cells treated with 0.33 µM nocodazole were stained with anti-ARHGEF17 antibodies (green) and ACAs (red), and DNA was counterstained with Hoechst 33342 (blue). (insets) High magnification of sister chromosomes. Dotted lines show the segmented centromeres. Bars: (main) 5 µm; (inset) 0.5 µm. (G) Quantitative analysis of the expression level of other checkpoint proteins at individual sister kinetochores. (left) Localization of Zwint-1, KNL1, or Ndc80 in si(Scrambled) or si(hARHGEF17) knockdown conditions. (insets) High magnification of kinetochores. Black lines outline the segmented chromosomes. Bars: (main) 10 µm; (inset) 0.5 µm. (right) Box plots comparing the mean intensity ratio between target kinetochore proteins (Zwint-1, KNL1, and Ndc80) and CENP-A at >500 individual kinetochores/three independent experiments in prometaphase in si(Scrambled) and a si(hARHGEF17) knockdown conditions normalized to si(Scrambled) in each condition. Boxes show median, 25–75%; whiskers show 1.5× interquartile range.Sister kinetochores were automatically segmented and analyzed by Fiji software with a custom Jython script (see Materials and methods). Bars, 5 µm. ARHGEF17 depletion caused no mislocalization of inner kinetochore protein Ndc80, but did of inner and linker kinetochore proteins, KNL1 and Zwint-1, whose kinetochore targeting is believed to be independent of Mps1 kinase (Maciejowski et al., 2010; Santaguida et al., 2010). This could either be a secondary consequence of the loss of outer kinetochore and checkpoint proteins or alternatively point to an additional Mps1 independent function for ARHGEF17 at the kinetochore. (H) Rescue of hARHGEF17 knockdown polylobed phenotype by ARHGEF17 fragments. Bar plots comparing polylobed percentage of si(Scrambled) and si(hARHGEF17) knockdown normalized to si(Scrambled) from >1,300 HeLa Kyoto cells stably expressing H2B-mCherry with or without the hARHGEF17 fragments as a rescue construct/three independent experiments. Bar graphs show mean ± SD. Cells were automatically segmented and analyzed with CellCognition. *, $P < 0.05$; **, $P < 0.01$ by two-tailed unpaired Student's *t* test, compared with si(hARHGEF17) (B) or si(hMad2) (C) knockdown without a rescue construct (B and C), si(Scrambled) (G), or si(hARHGEF17) knockdown without a rescue fragment (H).

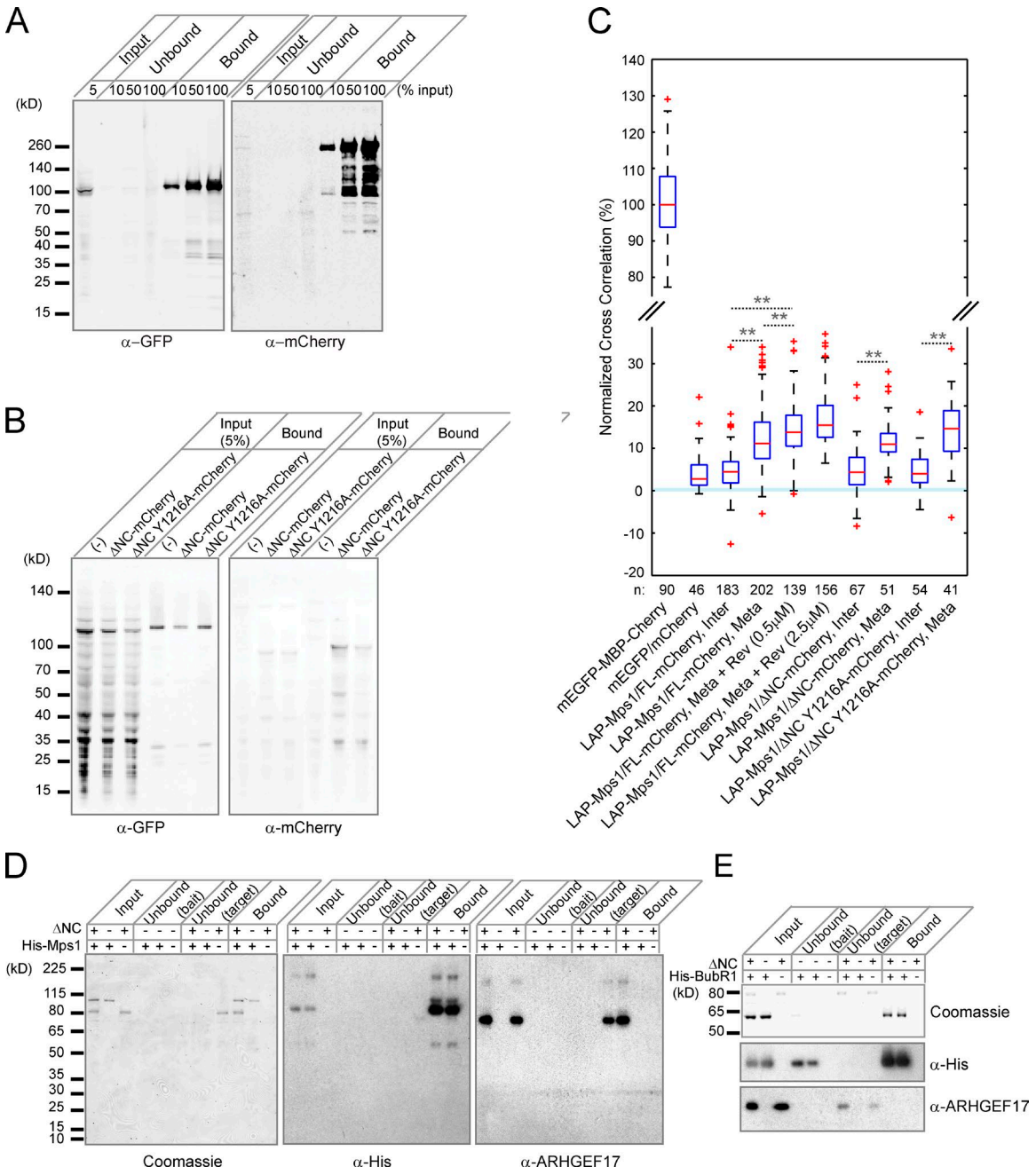

Figure S3. **ARHGEF17 and Mps1 interaction.** (A) Uncropped version of the Western blots shown in the main figures (Fig. 4 A). (B) Uncropped version of the Western blots shown in the main figures (Fig. 4 D). (C) Normalized cross correlation by FCCS in the cytoplasm of HeLa Kyoto cells coexpressing either EGFP and mCherry in fusion (EGFP-MBP-mCherry), EGFP and mCherry, or ARHGEF17-mCherry (FL-mCherry) and LAP-Mps1 with or without 0.5 or 2.5 μM reversine treatment in interphase (Inter) or mitosis (Meta) or ΔNC-mCherry and LAP-Mps1, or ΔNC Y1216A-mCherry and LAP-Mps1 in interphase or mitosis. Reversine was added 0.5 h before imaging to cells synchronized in metaphase by prior treatment with 20 μM MG132. Boxes show median, 25–75%; whiskers show 1.5× interquartile range. **, $P < 0.01$ by two-tailed unpaired Student's *t* test, compared with interphase or between metaphase and metaphase with reversine treatment. (D) Uncropped version of the Western blots shown in the main figures (Fig. 4 G). (E) In vitro pull-down of the ARHGEF17 fragments with BubR1. His-tagged BubR1 (kinase domain; bait) and untagged ARHGEF17 fragments (ΔNC; target) were precipitated using His-tag binding protein coupled with magnetic beads. Input, supernatants (Unbound), and precipitates (Beads) were analyzed by Western blotting with anti–His-tag (middle) and anti-ARHGEF17 (bottom) antibodies. Staining with Coomassie brilliant blue was used as an internal control of the protein in each condition.

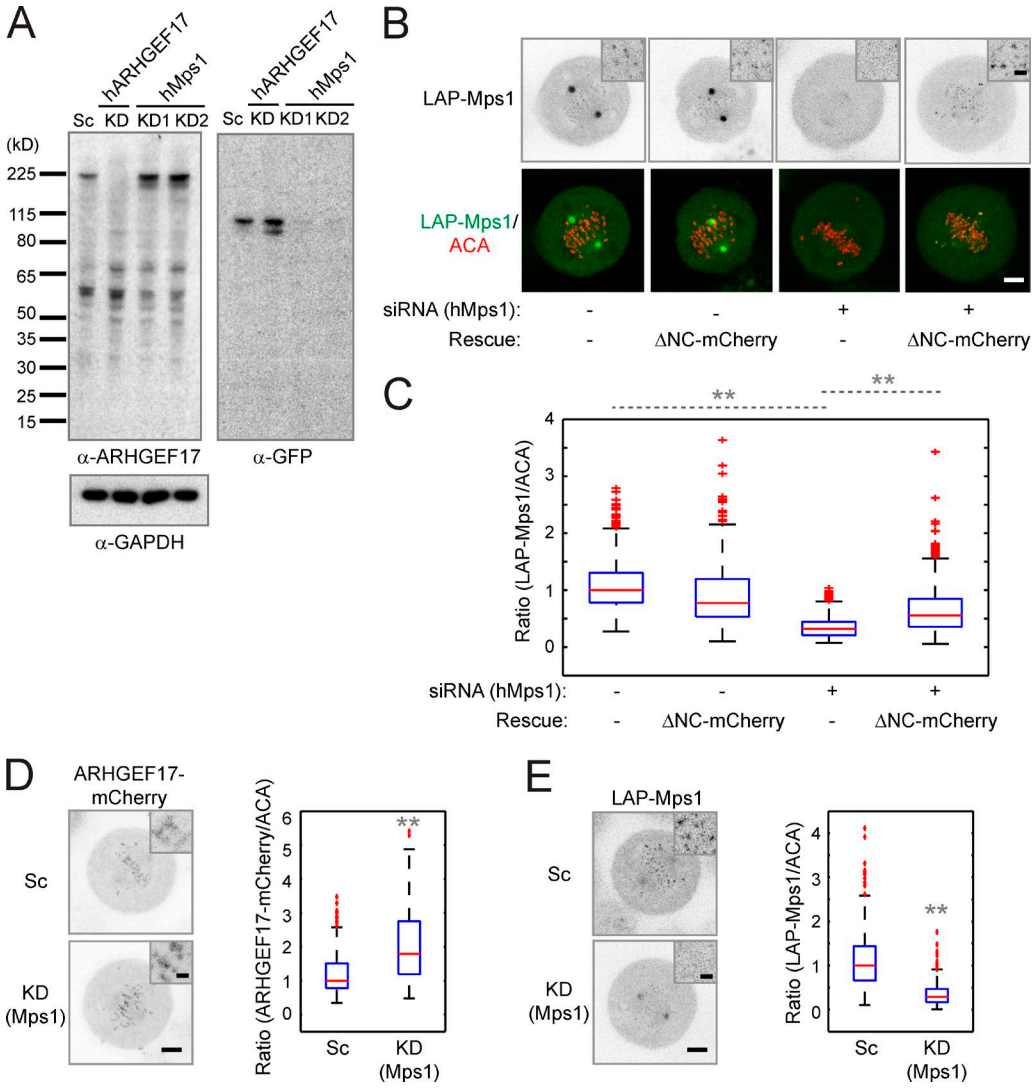

Figure S4. **ARHGEF17 is required for kinetochore targeting of Mps1.** (A) Immunoblot analysis of the protein expression level of hMps1 fused with LAP-tag and the endogenous hARHGEF17 48 h after siRNA transfection in si(Scrambled) (Sc), si(hARHGEF17) knockdown (KD), or si(hMps1; KD1, KD2) knockdown (KD) conditions detected by ARHGEF17 (left) and GFP (right) antibodies. GAPDH was used as a loading control. (B) Immunofluorescence images of hMps1 fused with LAP-tag at kinetochores in MG132-treated metaphase cells. Overlay shows Mps1 (green) and ACA (red) in si(Scrambled) and si(hARHGEF17) KD conditions with or without ARHGEF17-ΔNC expression as a rescue construct. (insets) High magnification of kinetochores. Bars: (main) 5 µm; (inset) 1 µm. (C) Quantitative ratiometric analysis of LAP-tagged Mps1. Box plot comparing the mean intensity ratio between Mps1 and ACA at >800 individual kinetochores/three independent experiments in each condition. Boxes show median, 25–75%; whiskers show 1.5× interquartile range. Sister kinetochores were automatically segmented and analyzed by Fiji software with a custom Jython script. (D and E) (left) Immunofluorescence images of endogenous hARHGEF17 (D) and hMps1 fused with LAP-tag (E) at kinetochores in MG132-treated metaphase cells with or without hMps1. (insets) High magnification of kinetochores. Bars: (main) 5 µm; (inset) 1 µm. (right) Quantitative ratiometric analysis of hARHGEF17 and LAP-tagged Mps1. Box plots comparing the mean intensity ratio between hARHGEF17 (D) or LAP-tagged Mps1 (E) and ACA at >1,000 individual kinetochores/three independent experiments in each condition. Boxes show median, 25–75%; whiskers show 1.5× interquartile range. **, $P < 0.01$ by two-tailed unpaired Student's *t* test, compared with si(Scrambled) (D and E), si(Scrambled) without a rescue fragment, or between si(hMps1) knockdown with or without a rescue fragment (C). Sister kinetochores were automatically segmented and analyzed by Fiji software with a custom Jython script.

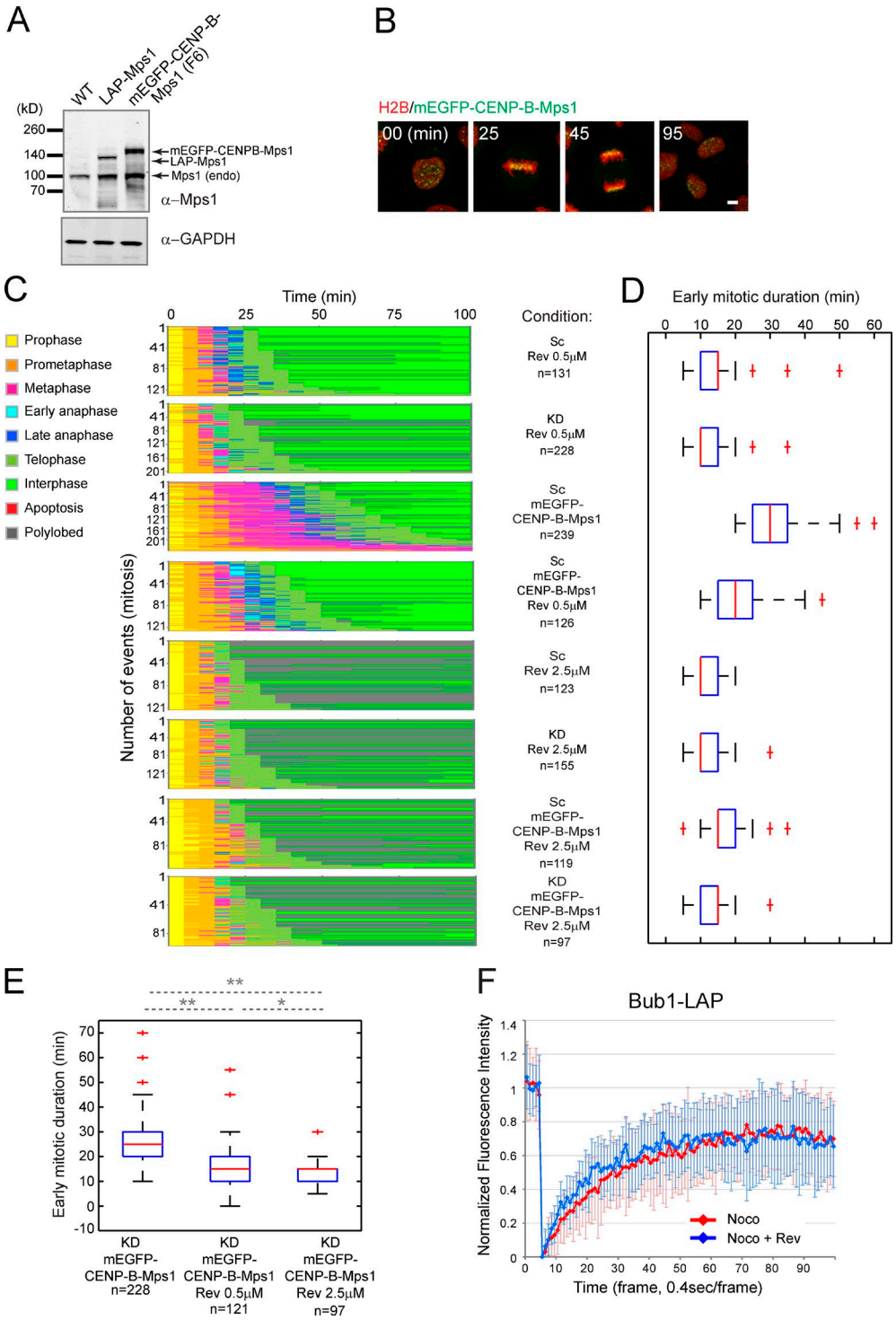

Figure S5. **Constitutive localization of Mps1 rescues the effect of ARHGEF17 knockdown during mitosis.** (A) Immunoblot analysis of the expression level of endogenous Mps1, LAP-tagged Mps1 (LAP-Mps1), and mEGFP-CENP-B-Mps1 in HeLa Kyoto cells with anti-Mps1 antibodies. GAPDH was used as a loading control. WT, wild-type. (B) Time series showing HeLa Kyoto cells stably expressing H2B-mCherry (red) and mEGFP-CENP-B-Mps1 (green). Bars, 5 μm. (C) Phenotypic rescue assay by artificial kinetochore tethering of Mps1 in the presence or absence of ARHGEF17. Mitotic events were automatically extracted in si(Scrambled) (Sc) or si(hARHGEF17) knockdown (KD) in HeLa Kyoto cells stably expressing H2B-mCherry and mEGFP-CENP-B-Mps1 as a rescue construct with or without 0.5 or 2.5 μM reversine treatment. Colors indicate H2B-mCherry morphology classes. (D) Quantitative analysis of early mitotic duration. Box plot comparing the sum duration of prometaphase and metaphase from >30 events/three independent experiments in each condition. Boxes show median, 25–75%; whiskers show 1.5× interquartile range. (E) Quantitative analysis of early mitotic duration with or without a different dose of 0.5 or 2.5 μM reversine treatment. Box plot comparing the sum duration of prometaphase and metaphase from 30 events/three independent experiments in each condition. Boxes show median, 25–75%; whiskers show 1.5× interquartile range. **, $P < 0.01$; *, $P < 0.05$ by two-tailed unpaired Student's *t* test, compared with no reversine treatment or between 0.5 and 2.5 μM reversine treatment. (F) FRAP analysis of Bub1 (Bub1-LAP) at kinetochore in nocodazole-treated mitotic cell with or without reversine treatment. Images were acquired every 0.4 s for 40 s (100 frames). FRAP curves were normalized between 1 (prebleach value) and 0 (postbleach value) and plotted over time. Mean ± SD of >30 individual cells in each condition.

Table S1. **List of siRNAs**

siRNA	Sequence
Scrambled	
Sense	5′-AAUCAGUUUGGGAAGAUGCtt-3′
Antisense	5′-GCAUCUUCCCAAACUGAUUtt-3′
Human ARHGEF17	
Sense	5′-GCUCCCUAUUGGAUCAGGAtt-3′ (1 and 4 having chemical modifications)
Antisense	5′-UCCUGAUCCAAUAGGGAGCtt-3 (1 and 4)
Sense	5′-GGGAUAUCAGGAGGUUAUUtt-3′ (2)
Antisense	5′-AAUAACCUCCUGAUAUCCCtt-3′ (2)
Sense	5′-GGACGACGACCUAUGGUCUtt-3′ (3)
Antisense	5′-AGACCAUAGGUCGUCGUCCtt-3′ (3)
Mouse ARHGE17	
Sense	5′-GUACCACCCUGAAACGAAAtt-3′
Antisense	5′-UUUCGUUUCAGGGUGGUACag-3′
Human Mad2	
Sense	5′-CGCCUUCGUUCAUUUACUATT-3′
Antisense	5′-UAGUAAAUGAACGAAGGCGga-3′
Human Mps1	
Sense	5′-GGUUGUGCCUGGAUCUAAAtt-3′ (1)
Antisense	5′-UUUAGAUCCAGGCACAACCaa-3 (1)
Sense	5′-GAUAGUUACCGGAACGAAAtt-3′ (2)
Antisense	5′-UUUCGUUCCGGUAACUAUCaa-3′ (2)

References

Maciejowski, J., K.A. George, M.-E. Terret, C. Zhang, K.M. Shokat, and P.V. Jallepalli. 2010. Mps1 directs the assembly of Cdc20 inhibitory complexes during interphase and mitosis to control M phase timing and spindle checkpoint signaling. *J. Cell Biol.* 190:89–100. http://dx.doi.org/10.1083/jcb.201001050

Santaguida, S., A. Tighe, A.M. D'Alise, S.S. Taylor, and A. Musacchio. 2010. Dissecting the role of MPS1 in chromosome biorientation and the spindle checkpoint through the small molecule inhibitor reversine. *J. Cell Biol.* 190:73–87. http://dx.doi.org/10.1083/jcb.201001036